

# Thermometry in dual quantum dot set-up with staircase ground state configuration

Sagnik Banerjee<sup>1</sup> and Aniket Singha<sup>2</sup>

<sup>1</sup>*Department of Electronics and Telecommunication Engineering,  
Jadavpur University, Jadavpur-700032, India*

<sup>2</sup>*Department of Electronics and Electrical Communication Engineering,  
Indian Institute of Technology Kharagpur, Kharagpur-721302, India*

We propose and investigate thermometry of a setup employing dual quantum dots with staircase ground state configuration. The stair-case ground state configuration actuates thermally controlled inelastic tunnelling, which translates into a temperature sensitive conductance, thereby inducing thermometry. The performance of the set-up is then analyzed employing quantum master equation (QME) for such systems in the sequential tunnelling regime. In particular, it is demonstrated that the system performance, in terms of temperature sensitivity and efficiency, is maximum in the regime of low temperature, making such system suitable for cryogenic thermometry. The proposed set-up can pave the path towards realization of high performance cryogenic nano temperature sensors.

## I. INTRODUCTION

Cryogenic thermometry has recently attracted significant attention with particular focus towards nano-scale systems. Electronic thermometry is actuated via temperature-induced control of electronic transport, which has manifested in the form of nano-scale thermoelectric engines [1–26], refrigerators [27–38], transistors [39–46] and rectifiers [47–52]. Theoretical investigation of cryogenic nano-thermometers employing quantum dots and quantum point contacts has been of immense interest recently due to their applications in the temperature regime of a few Kelvin. Despite such technology being in their infant stages, tremendous effort is being geared to enhance the performance of such set-ups in chip level systems.

In this paper, we propose and investigate cryogenic thermometry in a set-up employing dual quantum dots with staircase ground state configuration. The quantum dots are embedded in a nano-wire like structure. An equivalent set-up with multiple quantum dots was conceived earlier in literature as a means to optimize heat harvesting [53]. The energy difference between adjacent dot ground-states actuates inelastic process assisted tunneling, accompanied by energy absorption or emission. Thus, any change in the system temperature impacts the intensity of inelastic phenomena and thus induces a change in conductance. It is demonstrated that the thermometry performance in terms of temperature sensitivity and efficiency is optimal in the low-temperature regime, making such a set-up extremely suitable for cryogenic applications.

This paper is organized as follows. In Sec II we elaborate on the proposed system configuration. Next, in Sec III, we discuss the electronic transport formulation employed to analyze the thermometry performance of the proposed set-up. Sec IV elaborates on the performance and operating regime of the proposed set-up. Finally, we conclude the paper briefly in Sec V

## II. PROPOSED DEVICE STRUCTURE

The set-up proposed in this paper is shown in Fig. 1, and consists of two tunnel-coupled quantum dots  $S_1$  and  $S_2$ , which can exchange electrons with the reservoir  $L$  and  $R$  respectively. The coupling between the dot  $S_1(S_2)$  and reservoir  $L(R)$  is denoted by  $\gamma_c$ . The dots  $S_1$  and  $S_2$  are tunnel-coupled to each other and share a staircase ground state configuration with  $E_{S_2} = E_{S_1} + \delta E$ . In the weak inter-dot coupling limit, a stair-case ground state configuration with  $\delta E \gg \gamma_c$  suppresses electronic transport via elastic processes. Hence, any tunnelling of electrons between the dots has to be accompanied by an absorption or emission of an energy packet  $\delta E$ . A change in system temperature alters inelastic tunnelling probability between the dots, thereby modulating the current flow and exhibiting temperature sensitivity.

## III. ANALYSIS METHODOLOGY AND TRANSPORT FORMULATION

In the setup under consideration, the rate of inelastic absorption (emission) assisted tunnelling between two dots is denoted by  $\gamma_{ph}^{abs(em)}$ . The rate of elastic tunnelling ( $\gamma_{el}$ ) is assumed negligible due to the stair-case ground state configuration. In the typical situation of thermal equilibrium of lattice vibration, the rate of inelastic process assisted electronic tunnelling via energy absorption (emission) is dependent on the phonon number ( $N_{ph}$ ) associated with the energy difference  $\delta E$ . Thus, the rate of inelastic tunnelling ( $\gamma_{ph}^{abs(em)}$ ) between adjacent quantum dots can thus be written as,

$$\gamma_{ph}^{abs(em)} = t_{ph} \times \left( N_{ph} + \frac{1}{2} - (+)\frac{1}{2} \right), \quad (1)$$

where  $t_{ph}$  is a constant proportional to the inelastic process assisted coupling between adjacent quantum dots

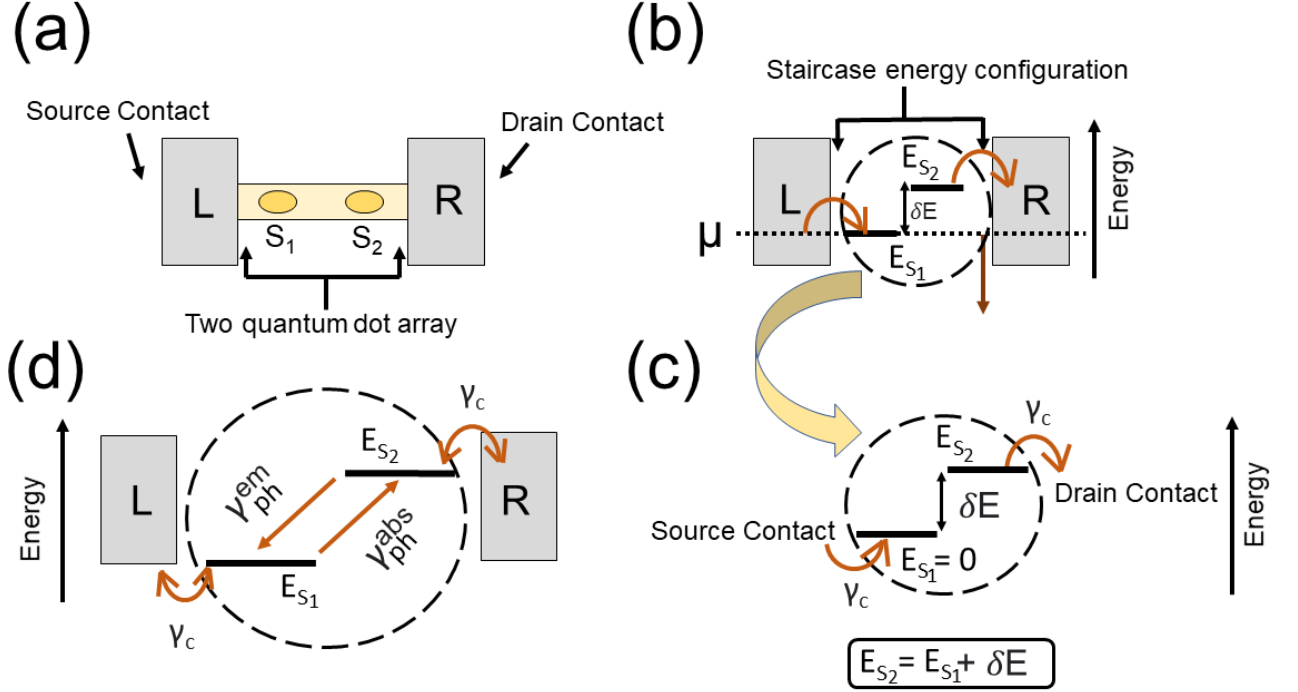


FIG. 1. Schematics of the proposed thermometer consisting of an array of two quantum dots with stair-like ground state energy configuration. (a) The proposed device is realized by embedding two quantum dots in a horizontal array, on a nanowire-like structure. (b) Illustrative diagram of the stair-like ground energy configuration of two dots. (c) A zoom into the schematics, highlighting the energy levels. The ground state energy of the first dot ( $E_{S_1}$ ) has been assumed to be zero. The equilibrium Fermi level is also aligned to  $E_{S_1}$ . (d) An intuitive diagram representing the electron transport between the two adjacent quantum dots via energy absorption and emission. The coupling of the left (right) contacts with respective quantum dots has also been indicated.

[30, 53]. We assume the limit of weak coupling and low-temperature to investigate the system under consideration such that electronic transport processes via cotunneling and higher order tunneling processes, as well as via higher excited states of the quantum dots can be neglected. In the case of thermal equilibrium, the phonon number ( $N_{ph}$ ) associated with energy  $\delta E$  is given by,

$$N_{ph} = [\exp(\delta E/k_B T) - 1]^{-1}, \quad (2)$$

To evaluate the thermometry performance, we employ the quantum master equation (QME) approach for such systems in the sequential transport regime to calculate the ground state occupancy probability [30]. Under thermal equilibrium of lattice vibration, the temporal dynamics of ground state occupancy probability, denoted by  $P_1$  and  $P_2$  for the dots  $S_1$  and  $S_2$  respectively, can be given

by the following set of equations:

$$\frac{dP_1}{dt} = \gamma_c f_L (1 - P_1) + (\gamma_{ph}^{em} + \gamma_{el}) P_2 (1 - P_1) - (\gamma_{ph}^{abs} + \gamma_{el}) P_1 (1 - P_2) - \gamma_c P_1 (1 - f_L) \quad (3)$$

$$\frac{dP_2}{dt} = (\gamma_{ph}^{abs} + \gamma_{el}) P_1 (1 - P_2) + \gamma_c f_R (1 - P_2) - \gamma_c P_2 (1 - f_R) - (\gamma_{ph}^{em} + \gamma_{el}) P_2 (1 - P_1), \quad (4)$$

where  $f_L$  and  $f_R$  denote the occupancy probability of the reservoirs  $L$  and  $R$  at energy  $E_{S_1}$  and  $E_{S_2}$  respectively. Assuming quasi-Fermi statistics for electron occupancy at the reservoirs,  $f_{L(R)}$  can be written as

$$f_{L(R)} = \left( 1 + \exp \left\{ \frac{E_{S_1(S_2)} - \mu_{L(R)}}{k_B T} \right\} \right)^{-1}, \quad (5)$$

where  $\mu_{L(R)}$  represents the quasi-Fermi energy levels of the reservoir  $L(R)$ . Under the condition of quasi-equilibrium among electronic population in the reservoir  $L$  and  $R$ , the quasi-Fermi energy in the respective reservoirs,  $\mu_{L(R)}$  may be written as  $\mu_{L(R)} = \mu + (-)V/2$ , where  $\mu$  is the equilibrium Fermi-energy throughout the entire

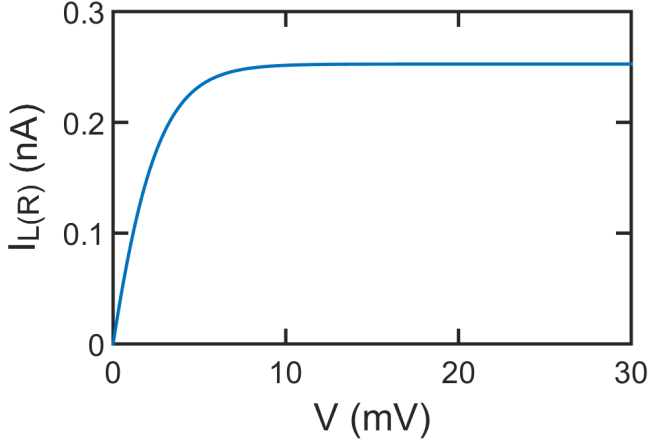


FIG. 2. Variation in the reservoir-to-dot electronic current with the applied bias across the array of two quantum dots. As already mentioned to be stair-case configured, the ground states of the dots  $E_{S_1}$  and  $E_{S_2}$  are assumed to be separated by an energy gap of  $\delta E = 10k_B$  (See Fig. 1).  $E_{S_1}$  is assumed to be aligned to  $\mu$ , and is set as reference *zero*. We choose the system temperature as 10K.

set-up, and  $V$  is the applied bias voltage with positive and negative poles connected to reservoir  $R$  and  $L$  respectively. Without loss of generality, the ground-state energy of the first dot  $E_{S_1}$  is set as *zero*. In such a case, the quasi-Fermi functions  $f_L$  and  $f_R$  can be written as:

$$f_L = \left( 1 + \exp \left\{ \frac{-(\mu + V/2)}{k_B T} \right\} \right)^{-1}$$

$$f_R = \left( 1 + \exp \left\{ \frac{\delta E - (\mu - V/2)}{k_B T} \right\} \right)^{-1} \quad (6)$$

Under steady state conditions,  $\frac{dP_{1(2)}}{dt} = 0$ . The set of differential Eqs. (3)-(4) are solved in steady state conditions using Newton-Raphson method to obtain the dot-occupancy probabilities. On calculation of the steady-state occupancy probabilities, the electronic current flowing out-of (into) the left (right) reservoirs can be written as:

$$I_{L(R)} = \frac{2q^2}{h} [\gamma_c (1 - P_{1(2)}) f_{L(R)} - \gamma_c (1 - P_{2(1)}) f_{L(R)}], \quad (7)$$

where,  $I = I_L = -I_R$ . In Eq. 7, factor of 2 is introduced to account for the spin degeneracy of electrons.

In the aspect of nano-scale thermometry, two parameters that may be employed to gauge the performance of the proposed set-up are temperature sensitivity and efficiency (temperature sensitivity per unit power dissipation). We define the thermometer sensitivity ( $\chi$ ) as the rate of change of electronic current between  $L$  and  $R$ , with the system temperature  $T$ .

$$\chi = \left( \frac{dI}{dT} \right) \quad (8)$$

The efficiency ( $\Lambda$ ) of the thermometer is dependent on the sensitivity and power dissipation as:

$$\Lambda = \chi/P, \quad (9)$$

where the power dissipation  $P$  across the thermometer is defined as:

$$P = V \times I, \quad (10)$$

$I$  being the electronic current across the set-up and  $V$  is the applied bias voltage. It should be noted that the parameter  $\Lambda$  defined here is not the true efficiency related to energy conversion, as in the of heat engine. Hence, the parameter  $\Lambda$  in this case is not limited to the maximum value of unity.

#### IV. RESULTS

In this section, we discuss the performance and the operating regime of the proposed thermometer. To investigate the proposed thermometer, we consider the limit  $\delta E \gg \gamma_c$ , where elastic tunneling remains suppressed ( $\gamma_{el} \approx 0$ ) due to staircase ground state configuration. Without loss of generality, we assume  $\gamma_c = 10\mu\text{eV}$  and  $t_{ph} = 1\mu\text{eV}$ . Such order of coupling parameter has been obtained from a recent experimental demonstration of non-local heat engine by Thierschmann *et. al.*[22], and restrict electronic transport in the weak coupling limit, where the rate of co-tunnelling and higher order tunnelling processes can be neglected and electronic flow can be considered to be confined in the sequential tunnelling regime. The assumption of the sequential electronic transport validates the use of quantum master equation (QME) for the analysis and performance investigation of the proposed set-up.

Fig. 2 depicts the variation in electronic current with the applied bias across the setup. To investigate the performance of the proposed set-up, we choose a bias voltage which results in the maximum saturation current. Such a choice also results in maximum possible sensitivity that can be obtained from the thermometer and renders noise robustness against any voltage fluctuation. For all the results that follow, the applied bias voltage is taken to be  $V = 15\text{mV}$ .

Fig. 3(a) demonstrates the variation in sensitivity with temperature ( $T$ ) and equilibrium Fermi potential ( $\mu$ ), for  $\delta E = 5k_B$  (0.43meV). This can be explained as follows. Initially when  $k_B T \ll \delta E$ , the phonon number  $N_{ph}$  is almost zero and increases at a very slow rate resulting in very low probability of electronic tunnelling via inelastic absorption and emission. This results in low value of electronic current and hence, temperature sensitivity. With increase in temperature, the optical phonon number  $N_{ph}$  gradually increases resulting in an increase in temperature sensitivity. As  $k_B T$  becomes comparable to  $\delta E$ , the rate of electronic tunnelling via both inelastic absorption and emission increases with

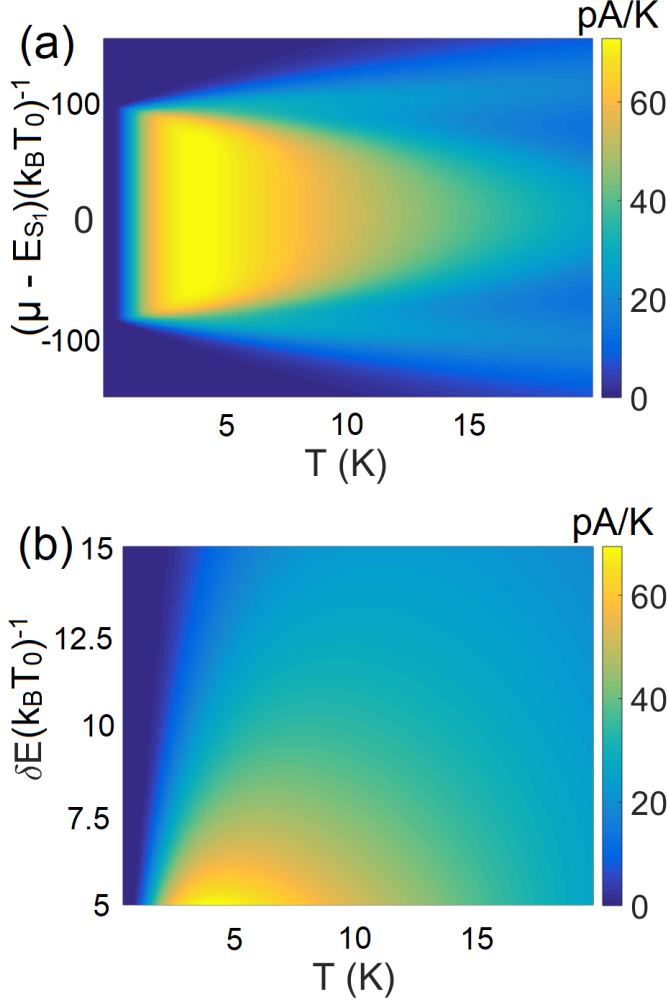


FIG. 3. Colour plots demonstrating the operation regime of the proposed setup. Variation in temperature sensitivity with (a) equilibrium Fermi potential ( $\mu$ ) and temperature  $T$  (b) ground state energy difference between the two dots ( $\delta E$ ) and temperature  $T$ . For both cases, the applied bias across the setup is chosen to be  $V = 15mV$ . In the above plots,  $T_0 = 1K$

$T$ . The rate of increase of current depends on the temperature dynamics of  $\frac{\gamma_{ph}^{abs}}{\gamma_{ph}^{em}}$ . The gradual decrease, followed by saturation of the ratio  $\frac{\gamma_{ph}^{abs}}{\gamma_{ph}^{em}}$  with  $T$ , results in the gradual decrease in sensitivity followed by saturation as  $k_B T$  becomes comparable to and greater than  $\delta E$ . Moreover, we note that the set-up performs optimally for a finite energy range around  $\mu - E_{S1} = 0$ . As  $\mu$  deviates from  $E_{S1}$  beyond a certain limit, the temperature sensitivity gradually becomes zero due to a net decrease in electronic tunnelling between reservoirs  $L$  and  $R$ . Fig. 3(b) demonstrates the variation in sensitivity with temperature ( $T$ ) and ground state misalignment ( $\delta E$ ) between the adjacent dots, assuming  $\mu$  to be aligned with  $E_{S1}$ . As expected, the sensitivity decreases mono-

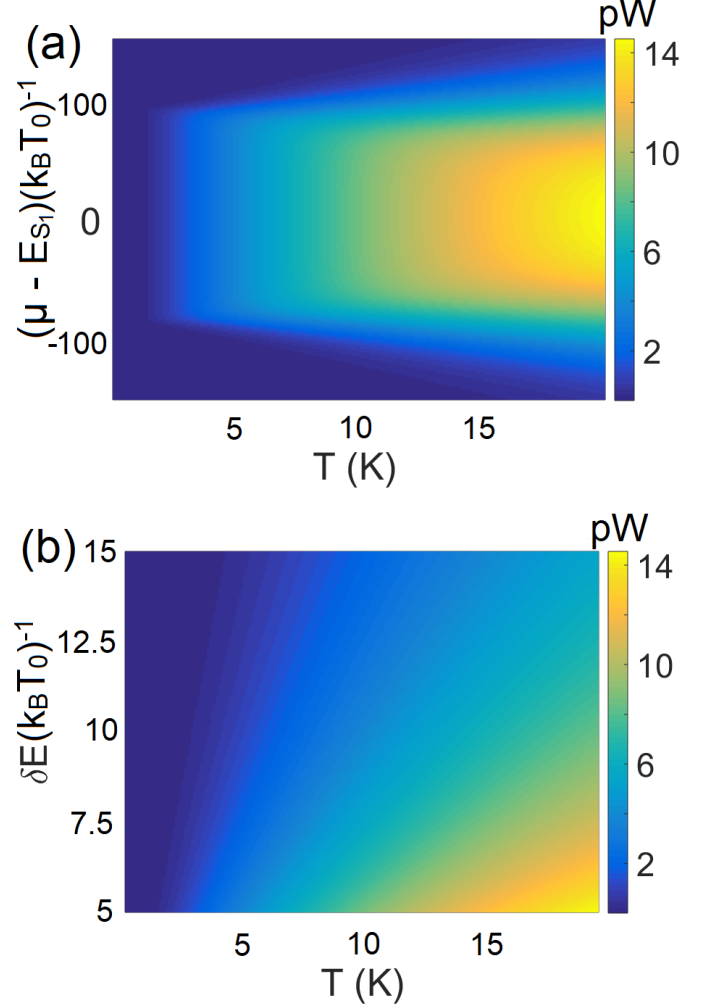


FIG. 4. Colour plots demonstrating the power dissipation across the proposed setup. Variation in power dissipated with (a) equilibrium Fermi potential ( $\mu$ ) and temperature  $T$  (b) ground state energy difference between the two dots ( $\delta E$ ) and temperature  $T$ . For both cases, the applied bias across the setup is chosen to be  $V = 15mV$ . In the above plots,  $T_0 = 1K$

tonically with increase in  $\delta E$ . This can be explained as follows. An increase in  $\delta E$  reduces the rate of inelastic inter-dot tunnelling resulting in an overall decrease in current, and hence sensitivity. It should be noted that although the sensitivity increases with decrease in  $\delta E$ , a reduction in  $\delta E$  beyond a certain limit might result in the actuation of elastic inter-dot tunnelling, which results in a deterioration of sensitivity and enhancement in dissipated power, degrading the overall performance of the set-up (see Appendix A).

Fig. 4(a) demonstrates the variation in dissipated power across the set-up with temperature  $T$  and equilibrium Fermi energy  $\mu$  at  $\delta E = 5k_B$  ( $0.43meV$ ). As discussed earlier, an increase in temperature results in an enhancement in inelastic process assisted tunnelling

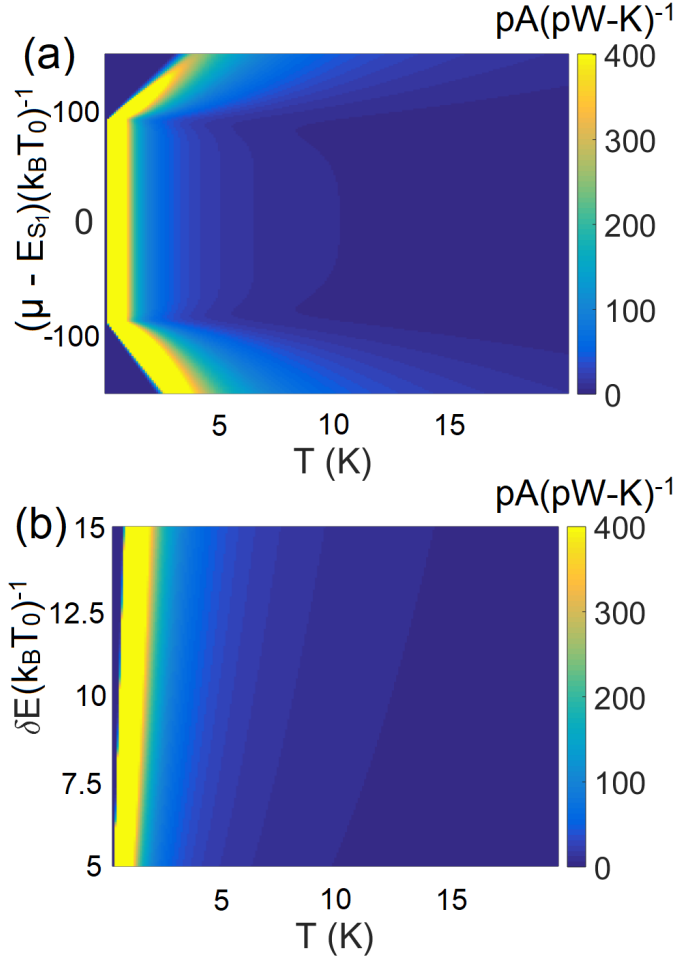


FIG. 5. Colour plots demonstrating the performance of the proposed setup. Variation in efficiency with (a) equilibrium Fermi potential ( $\mu$ ) and temperature  $T$  (b) ground state energy difference between the two dots ( $\delta E$ ) and temperature  $T$ . For both cases, the applied bias across the setup is chosen to be  $V = 15mV$ . In the above plots,  $T_0 = 1K$

due to increase in phonon number ( $N_{ph}$ ). Thus, dissipated power increases as the current increases with temperature  $T$  due to an increase in electronic tunnelling rate. Fig. 4(b) shows the variation in power dissipated across the set-up, with temperature  $T$  and ground state energy difference  $\delta E$  between adjacent quantum dots. As discussed earlier, lower values of  $\delta E$  and higher  $T$  result in a higher electronic current (due to increase in phonon number  $N_{ph}$ ) and hence, increase the dissipated power.

Fig. 5(a) demonstrates the variation in efficiency (sensitivity per unit power dissipation) of the proposed thermometer with temperature  $T$  and equilibrium Fermi energy  $\mu$ . It should be noted that the maximum efficiency for the proposed set-up occurs in the low temperature regime making such set-ups extremely attractive for low temperature thermometry. The system efficiency decreases with  $T$  due to both decrease in sensitivity and

increase in power dissipation. Fig. 5(b) demonstrates the variation in efficiency with temperature  $T$  and ground state energy difference  $\delta E$ . The overall efficiency, as noted from Fig. 5(b), doesn't deviate strongly with  $\delta E$ .

## V. CONCLUSION

To conclude, in this paper we have proposed and analysed a set-up that employs dual quantum dots with staircase ground state configuration to achieve thermometry. The performance of the proposed set-up is actuated by an increase in inelastic absorption (emission) mediated electronic tunnelling with temperature, resulting in a temperature sensitive conductance. It was demonstrated that the set-up offers the maximum sensitivity, as well as efficiency, in the low temperature regime, rendering it suitable for deployment in the regime of tens of Kelvin. In this paper, we have analyzed the set-up in the limit of weak system-to-reservoir coupling and sequential electronic transport. It would be interesting to investigate the performance as the system is gradually tuned towards the strong coupling regime. Moreover, an investigation of the effect of Coulomb blockade on the thermometry performance of the proposed set-up also constitute an interesting direction. Such explorations are left for future research. Nevertheless, the set-up proposed in this paper may be employed to achieve high performance nano thermometers.

**Acknowledgments:** Aniket Singha would like to thank financial support from Sponsored Research and Industrial Consultancy (IIT Kharagpur) via grant no. IIT/SRIC/EC/MWT/2019-20/162, Ministry of Human Resource Development (MHRD), Government of India via Grant No. STARS/APR2019/PS/566/FS under STARS scheme and Science and Engineering Research Board (SERB), Government of India via Grant No. SRG/2020/000593 under SRG scheme.

## Appendix A: Effect of elastic inter-dot tunneling on the thermometry performance

Through out our discussion in the main text, we have neglected elastic tunneling processes between the two dots. Due to the staircase ground state configuration, elastic tunnelling remains suppressed in the limit of  $\delta E \gg \gamma_c$ . However, when  $\delta E$  becomes comparable to or less than  $\gamma_c$ , due to finite lifetime-broadening of the ground states, elastic inter-dot tunneling creeps in [54, 55] and begins to manifest itself as a deterioration in system performance. Elastic interdot tunneling is independent of system temperature and thus the electronic current mediated via elastic processes reduces the system efficiency in addition to decreasing the temperature sensitivity (Inelastic process assisted tunnelling now has



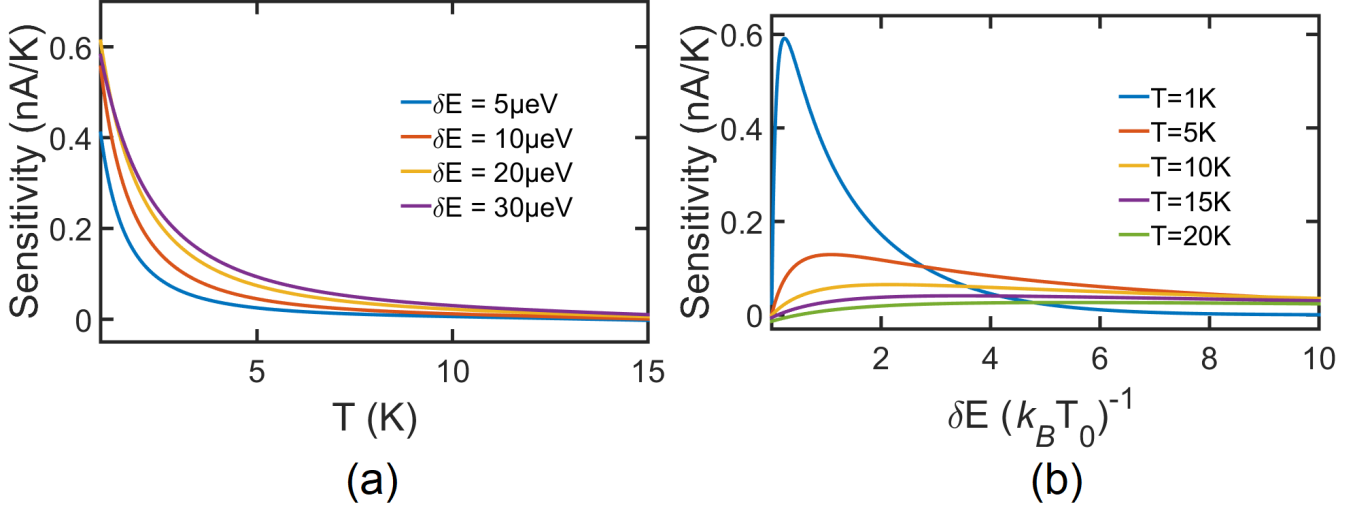


FIG. 6. Variation in (a) sensitivity with temperature  $T$ , for various values of ground state energy difference ( $\delta E$ ) (b) sensitivity with  $\delta E$ , for different temperature  $T$ . Here  $T_0 = 1\text{K}$ . The coupling between the left (right) contacts with respective quantum dots is assumed to be  $\gamma_c = 10\mu\text{eV}$ . For both cases, the voltage bias has been chosen to be  $V = 15\text{mV}$ .

to compete with elastic phenomena mediated tunneling). In the weak interdot coupling limit, the elastic tunnelling ( $\gamma_{el}$ ) between adjacent quantum dots can be given as [56],

$$\gamma_{el} = t^2 \times \left[ \frac{2\gamma_c}{(\delta E)^2 + (\gamma_c)^2} \right], \quad (\text{A1})$$

where  $\gamma_{el}$ ,  $\gamma_{abs(em)}$ ,  $\gamma_c$  have their usual meanings stated earlier in the main text and  $t$  is the inter-dot hopping parameter [54, 55]. To investigate the impact of elastic tunneling on the system performance, we solve the set of Eqns. 3-4, assuming  $t = 1\mu\text{eV}$  and all other parameters remaining the same.

Fig. 6(a) depicts the variation in sensitivity with tem-

perature  $T$  for different values of  $\delta E$  in the regime where  $\delta E$  is comparable to or less than  $\gamma_c$ . We note that in this regime the sensitivity decreases with a decrease in  $\delta E$ , a trend opposite to that noted in Fig. 3 ( $\delta E \gg \gamma_c$ ). The decrease in sensitivity with decrease in  $\delta E$  occurs due to an increase in the rate of elastic tunnelling ( $\gamma_{el}$ ) which gradually suppresses inelastic process assisted tunneling and thus reduces the system sensitivity. Fig. 6(b), illustrates the variation in sensitivity with  $\delta E$ , for different values of  $T$ . We note that the sensitivity increases as the  $\delta E$  is gradually decreased till the point  $\delta E$  becomes comparable to  $\gamma_c$ . When  $\delta E$  becomes comparable to and subsequently less than  $\gamma_c$ , the sensitivity decreases as elastic tunneling initiates and gradually starts dominating over inelastic process assisted tunneling.

- 
- [1] B. Sothmann, R. Sánchez, and A. N. Jordan, Thermoelectric energy harvesting with quantum dots, *Nanotechnology* **26**, 032001 (2014).
  - [2] A. Singha, A realistic non-local heat engine based on coulomb-coupled systems, *Journal of Applied Physics* **127**, 234903 (2020).
  - [3] G. Benenti, G. Casati, K. Saito, and R. S. Whitney, Fundamental aspects of steady-state conversion of heat to work at the nanoscale, *Physics Reports* **694**, 1 (2017), fundamental aspects of steady-state conversion of heat to work at the nanoscale.
  - [4] A. A. M. Staring, L. W. Molenkamp, B. W. Alphenaar, H. van Houten, O. J. A. Buyk, M. A. A. Mabesoone, C. W. J. Beenakker, and C. T. Foxon, Coulomb-blockade oscillations in the thermopower of a quantum dot, *Europhysics Letters (EPL)* **22**, 57 (1993).
  - [5] A. Dzurak, C. Smith, M. Pepper, D. Ritchie, J. Frost, G. Jones, and D. Hasko, Observation of coulomb blockade oscillations in the thermopower of a quantum dot, *Solid State Communications* **87**, 1145 (1993).
  - [6] T. E. Humphrey, R. Newbury, R. P. Taylor, and H. Linke, Reversible quantum brownian heat engines for electrons, *Phys. Rev. Lett.* **89**, 116801 (2002).
  - [7] O. Entin-Wohlman, Y. Imry, and A. Aharony, Three-terminal thermoelectric transport through a molecular junction, *Phys. Rev. B* **82**, 115314 (2010).
  - [8] R. Sánchez and M. Büttiker, Optimal energy quanta to current conversion, *Phys. Rev. B* **83**, 085428 (2011).
  - [9] A. Singha, S. D. Mahanti, and B. Muralidharan, Exploring packaging strategies of nano-embedded thermoelectric generators, *AIP Advances* **5**, 107210 (2015).
  - [10] B. Sothmann, R. Sánchez, A. N. Jordan, and M. Büttiker, Rectification of thermal fluctuations in a chaotic cavity

- heat engine, *Phys. Rev. B* **85**, 205301 (2012).
- [11] B. De and B. Muralidharan, Non-linear phonon peltier effect in dissipative quantum dot systems, *Scientific Reports* **8**, 5185 (2018).
  - [12] B. De and B. Muralidharan, Manipulation of non-linear heat currents in the dissipative anderson–holstein model, *Journal of Physics: Condensed Matter* **32**, 035305 (2019).
  - [13] B. De and B. Muralidharan, Thermoelectric study of dissipative quantum-dot heat engines, *Phys. Rev. B* **94**, 165416 (2016).
  - [14] A. Singha, Enhanced thermoelectric performance actuated by inelastic processes in the channel region, *Physica E: Low-dimensional Systems and Nanostructures* **117**, 113832 (2020).
  - [15] A. Singha and B. Muralidharan, Incoherent scattering can favorably influence energy filtering in nanostructured thermoelectrics, *Scientific Reports* **7**, 7879 (2017).
  - [16] B. Sothmann and M. Büttiker, Magnon-driven quantum-dot heat engine, *EPL (Europhysics Letters)* **99**, 27001 (2012).
  - [17] C. Bergenfeldt, P. Samuelsson, B. Sothmann, C. Flindt, and M. Büttiker, Hybrid microwave-cavity heat engine, *Phys. Rev. Lett.* **112**, 076803 (2014).
  - [18] R. Sánchez, B. Sothmann, and A. N. Jordan, Chiral thermoelectrics with quantum hall edge states, *Phys. Rev. Lett.* **114**, 146801 (2015).
  - [19] P. P. Hofer and B. Sothmann, Quantum heat engines based on electronic mach-zehnder interferometers, *Phys. Rev. B* **91**, 195406 (2015).
  - [20] B. Roche, P. Rouleau, T. Jullien, Y. Jompol, I. Farrer, D. A. Ritchie, and D. C. Glatli, Harvesting dissipated energy with a mesoscopic ratchet, *Nature Communications* **6**, 6738 (2015).
  - [21] F. Hartmann, P. Pfeffer, S. Höfling, M. Kamp, and L. Worschech, Voltage fluctuation to current converter with coulomb-coupled quantum dots, *Phys. Rev. Lett.* **114**, 146805 (2015).
  - [22] H. Thierschmann, R. Sánchez, B. Sothmann, F. Arnold, C. Heyn, W. Hansen, H. Buhmann, and L. W. Molenkamp, Three-terminal energy harvester with coupled quantum dots, *Nature Nanotechnology* **10**, 854 (2015).
  - [23] R. S. Whitney, R. Sánchez, F. Haupt, and J. Splettstoesser, Thermoelectricity without absorbing energy from the heat sources, *Physica E: Low-dimensional Systems and Nanostructures* **75**, 257 (2016).
  - [24] J. Schulenburg, A. Di Marco, J. Vanherck, M. Wegewijs, and J. Splettstoesser, Thermoelectrics of interacting nanosystems—exploiting superselection instead of time-reversal symmetry, *Entropy* **19**, 668 (2017).
  - [25] M. Josefsson, A. Svilans, A. M. Burke, E. A. Hoffmann, S. Fahlvik, C. Thelander, M. Leijnse, and H. Linke, A quantum-dot heat engine operating close to the thermodynamic efficiency limits, *Nature Nanotechnology* **13**, 920 (2018).
  - [26] R. Sánchez, J. Splettstoesser, and R. S. Whitney, Nonequilibrium system as a demon, *Physical Review Letters* **123**, 10.1103/physrevlett.123.216801 (2019).
  - [27] F. Giazotto, T. T. Heikkilä, A. Luukanen, A. M. Savin, and J. P. Pekola, Opportunities for mesoscopics in thermometry and refrigeration: Physics and applications, *Rev. Mod. Phys.* **78**, 217 (2006).
  - [28] J. P. Pekola and F. W. J. Hekking, Normal-metal-superconductor tunnel junction as a brownian refrigerator, *Phys. Rev. Lett.* **98**, 210604 (2007).
  - [29] A. Barman, S. Halder, S. K. Varshney, G. Dutta, and A. Singha, Realistic non-local refrigeration engine based on coulomb coupled systems (2020), [arXiv:2005.07966 \[physics.app-ph\]](https://arxiv.org/abs/2005.07966).
  - [30] A. Singha, Optimized peltier cooling via an array of quantum dots with stair-like ground-state energy configuration, *Physics Letters A* **382**, 3026 (2018).
  - [31] A. Singha and B. Muralidharan, Performance analysis of nanostructured peltier coolers, *Journal of Applied Physics* **124**, 144901 (2018).
  - [32] H. L. Edwards, Q. Niu, and A. L. de Lozanne, A quantum-dot refrigerator, *Applied Physics Letters* **63**, 1815 (1993), <https://doi.org/10.1063/1.110672>.
  - [33] J. R. Prance, C. G. Smith, J. P. Griffiths, S. J. Chorley, D. Anderson, G. A. C. Jones, I. Farrer, and D. A. Ritchie, Electronic refrigeration of a two-dimensional electron gas, *Phys. Rev. Lett.* **102**, 146602 (2009).
  - [34] Y. Zhang, G. Lin, and J. Chen, Three-terminal quantum-dot refrigerators, *Phys. Rev. E* **91**, 052118 (2015).
  - [35] J. V. Koski, A. Kutvonen, I. M. Khaymovich, T. Ala-Nissila, and J. P. Pekola, On-chip maxwell’s demon as an information-powered refrigerator, *Phys. Rev. Lett.* **115**, 260602 (2015).
  - [36] S. Mukherjee, B. De, and B. Muralidharan, Three terminal vibron coupled hybrid quantum dot thermoelectric refrigeration (2020), [arXiv:2004.12763 \[cond-mat.mes-hall\]](https://arxiv.org/abs/2004.12763).
  - [37] P. P. Hofer, M. Perarnau-Llobet, J. B. Brask, R. Silva, M. Huber, and N. Brunner, Autonomous quantum refrigerator in a circuit qed architecture based on a josephson junction, *Phys. Rev. B* **94**, 235420 (2016).
  - [38] R. Sánchez, Correlation-induced refrigeration with superconducting single-electron transistors, *Applied Physics Letters* **111**, 223103 (2017), <https://doi.org/10.1063/1.5008481>.
  - [39] J.-H. Jiang, M. Kulkarni, D. Segal, and Y. Imry, Phonon thermoelectric transistors and rectifiers, *Phys. Rev. B* **92**, 045309 (2015).
  - [40] B. Li, L. Wang, and G. Casati, Negative differential thermal resistance and thermal transistor, *Applied Physics Letters* **88**, 143501 (2006), <https://doi.org/10.1063/1.2191730>.
  - [41] K. Joulain, J. Drevillon, Y. Ezzahri, and J. Ordóñez-Miranda, Quantum thermal transistor, *Phys. Rev. Lett.* **116**, 200601 (2016).
  - [42] R. Sánchez, H. Thierschmann, and L. W. Molenkamp, Single-electron thermal devices coupled to a mesoscopic gate, *New Journal of Physics* **19**, 113040 (2017).
  - [43] R. Sánchez, H. Thierschmann, and L. W. Molenkamp, All-thermal transistor based on stochastic switching, *Phys. Rev. B* **95**, 241401 (2017).
  - [44] Y. Zhang, Z. Yang, X. Zhang, B. Lin, G. Lin, and J. Chen, Coulomb-coupled quantum-dot thermal transistors, *EPL (Europhysics Letters)* **122**, 17002 (2018).
  - [45] G. Tang, J. Peng, and J.-S. Wang, Three-terminal normal-superconductor junction as thermal transistor, *The European Physical Journal B* **92**, 27 (2019).
  - [46] B.-q. Guo, T. Liu, and C.-s. Yu, Quantum thermal transistor based on qubit-qutrit coupling, *Phys. Rev. E* **98**, 022118 (2018).

- [47] R. Scheibner, M. König, D. Reuter, A. D. Wieck, C. Gould, H. Buhmann, and L. W. Molenkamp, Quantum dot as thermal rectifier, *New Journal of Physics* **10**, 083016 (2008).
- [48] T. Ruokola and T. Ojanen, Single-electron heat diode: Asymmetric heat transport between electronic reservoirs through coulomb islands, *Phys. Rev. B* **83**, 241404 (2011).
- [49] A. Fornieri, M. J. Martínez-Pérez, and F. Giazotto, A normal metal tunnel-junction heat diode, *Applied Physics Letters* **104**, 183108 (2014), <https://doi.org/10.1063/1.4875917>.
- [50] J.-H. Jiang, M. Kulkarni, D. Segal, and Y. Imry, Phonon thermoelectric transistors and rectifiers, *Phys. Rev. B* **92**, 045309 (2015).
- [51] R. Sánchez, B. Sothmann, and A. N. Jordan, Heat diode and engine based on quantum hall edge states, *New Journal of Physics* **17**, 075006 (2015).
- [52] M. J. Martínez-Pérez, A. Fornieri, and F. Giazotto, Rectification of electronic heat current by a hybrid thermal diode, *Nature Nanotechnology* **10**, 303 (2015).
- [53] L. Li and J.-H. Jiang, Staircase quantum dots configuration in nanowires for optimized thermoelectric power, *Scientific Reports* **6**, 31974 (2016).
- [54] S. Datta, *Electronic Transport in Mesoscopic Systems* (Cambridge University Press, 1997).
- [55] S. Datta, *Quantum Transport: Atom to Transistor* (Cambridge Press, 2005).
- [56] A. Singha, Density matrix to quantum master equation (QME) model for arrays of coulomb coupled quantum dots in the sequential tunneling regime, *IOP SciNotes* **1**, 025204 (2020).